

Validation of two-fluid boiling flow model on the DEBORA benchmark experimental data

Aljoša Gajšek, Boštjan Končar, Matej Tekavčič, Andrej Prošek

Reactor Engineering Division, Jožef Stefan Institute

Jamova cesta 39

1000, Ljubljana, Slovenija

gajsek.aljosa@gmail.com, bostjan.koncar@ijs.si, matej.tekavcic@ijs.si, andrej.prosek@ijs.si

ABSTRACT

In this work simulations of 4 DEBORA experiments have been performed with ANSYS Fluent code in Eulerian two-fluid framework, using the standard wall boiling model. The cases varied by their inlet sub-cooling and consequently represented different boiling flow regimes. Temperature, void fraction, Sauter mean diameter and velocity profiles were compared with the experimental data. Preliminary analysis showed qualitatively good agreement of simulated-temperature and velocity profiles with DEBORA experiments, while more detailed study of boiling and inter-phase transfer parameters will be needed to better match the void fraction profiles and bubble diameter profiles. Mainly the simulated Sauter mean diameters also significantly over-estimated the measured values in the near-wall regions.

1 INTRODUCTION

With continuous development of three-dimensional multi-phase modelling capabilities, the numerical simulation of complex two-phase flows becomes feasible. In particular, the two-fluid model relying on phase-averaged equations has gained a lot of attention in the past decade due to its wide range of applicability and above all, as the model is applicable to industrial conditions. However, the two-fluid model approach requires many closure relations and a great diversity of sub-models has been developed. So far, it seems that none of them has reached a general level of applicability to any flow condition. It is clear that each set of sub-models needs to be validated against small-scale experimental data. In most cases, the authors use its own validation database, therefore the range of validity of their models is difficult to compare. An effort in this direction has been made in the frame of NEPTUNE project [1], supported by Commissariat à l'Énergie Atomique et aux Énergies Alternatives (CEA), Electricité de France (EdF), Framatome and Institut de Radioprotection et de Sûreté Nucléaire (IRSN), where the benchmark test has been launched trying to pave the way towards a unified method for testing and validation of two-fluid closure models based on publicly available experimental data. The first tests will be focused on high-pressure flow boiling in a simple tube geometry, performed in DEBORA experimental facility at CEA-Grenoble [2]. The DEBORA experiments provide a reliable database on local measurements of boiling phenomena in a simple vertical tube geometry with electrically heated wall. A turbulent boiling flow of Freon R12 or R134a has been used to mimic the high-pressure conditions, relevant for nuclear applications in Pressurized Water Reactors (PWR). The DEBORA benchmark exercise within the NEPTUNE project aims to provide to the Computational Multiphase Fluid Dynamics (CMFD) community a large database of available experimental data and will prepare the validation of simulation results provided by participants in an organised way. In the second phase, new experimental data will be provided and used for blind test exercise.

The Reactor engineering division of Jožef Stefan Institute decided to participate in this benchmark exercise, taking advantage of the many years of experience with modelling of

different types of multi-phase flows. In this work, the simulations of the open DEBORA boiling tests have been performed with the ANSYS Fluent code [3]. The simulation results are compared with the local measurements of radial profiles of void fraction, bubble size, liquid temperature and gas phase velocities.

2 DEBORA EXPERIMENTS

2.1 Simulated experimental cases

The simulations of four different cases were performed. Four cases with similar heat and mass fluxes but different inlet sub-cooling ($T_0 - T_{sat}$) were studied. Due to the limitation of experiment only some physical quantities could be measured at once [2]. The 8th series of experiments studied liquid temperature profiles at the end of the heated section, while the 29th series focused on gas velocity, void fraction and bubble diameter. During the individual measurement of the radial profile, inlet velocity, heat flux and inlet temperature could vary slightly, typically in the range of 0.1%. Additionally, the same quantities could vary up to a few percent (mostly for the heat flux) between the different experiments with the suggested constant initial value. Operating conditions of the selected experimental cases are presented in Table 1.

Table 1: Simulated experimental cases

Simulation id	Experiment Id	T_0 [°C]	$T_0 - T_{sat}$ [°C]	Mass flux [kg/m ² s]	Heat flux [kW/m ²]	Pressure [bar]
Debora 1	8G2P14W16Te29.5	29.47	-28.63	2009	73.90	14.60
Debora 2	29G2P14W16Te31.1	31.16	-26.92	2030	76.24	14.59
Debora 3	29G2P14W16Te35.3	36.16	-21.88	1999	75.80	14.58
Debora 4	29G2P14W16Te43.5	44.21	-13.76	2024	76.26	14.59

The selected experimental cases have similar operating conditions except for the inlet temperature. Debora 1 case was from 8th series and was chosen to validate the model's ability to describe the temperature profile. Debora 2, 3 and 4 were then selected to investigate the model's behaviour in different boiling flow regimes.

2.2 Properties of the working fluid R12

All chosen experiments were performed with dichlorodifluoromethane (R-12). Thermo-physical properties were extracted from [4].

For liquid phase isobaric temperature dependent data at the operating pressure were chosen, as the pressure dependencies were low. The vapour temperature was assumed to be at the saturation temperature in the entire domain, except for the near-wall cells, where this assumption could not be always satisfied. The saturation temperature in the boiling model was modelled as a pressure dependent value $T_{sat}(p)$.

3 MODELING APPROACH

3.1 Two-fluid model

The simulation was performed with Eulerian two-fluid model. It is assumed that both phases share the same pressure. Momentum, continuity and energy equations are solved separately for each phase [3].

3.2 Turbulence modelling

For turbulence the mixture model was used in which the turbulence is modelled as for a single phase with phase averaged mixture properties. The $k-\omega$ SST turbulence model was used [5]. Additionally, the effects of the dispersed gas phase to the liquid turbulence have been modelled. Two different modelling approaches have been tried. Troshko and Hassan [6] approach adds additional source term in the turbulence transport equation. Sato approach [7] however, models this effect as additional diffusion term directly in the momentum equation. Due to the better convergence, Sato model was used, with the model constant of 0.5.

3.3 Wall boiling model

Wall boiling considers the subcooled flow boiling regime up to saturation. Subcooled boiling describes the condition where the wall temperature is sufficiently high to trigger the boiling on the heated wall surface. The heat is transferred directly from the wall to the liquid, partly to heat up the liquid phase and partly to generate vapour bubbles. Condensation of the saturated vapour bubbles in the subcooled bulk also increase the average liquid temperature. Some energy might also be transferred directly from wall to the vapour. These mechanisms are the basis of Polytechnic Institute (RPI) models [8].

3.4 Heat flux partitioning model

According to the RPI model the total heat flux is partitioned into three components

$$\dot{q}_W = \dot{q}_C + \dot{q}_Q + \dot{q}_E, \quad (1)$$

where \dot{q}_W is the total wall heat flux, \dot{q}_C is convective heat flux, \dot{q}_Q is quenching heat flux and \dot{q}_E is evaporative heat flux. The heated wall surface is divided into the bubble influence area A_b , covered by bubbles and $(1 - A_b)$ covered by the liquid. Del Valle and Kenning's [9] model was used to model the bubble influence area A_b found in equation (2).

Convective heat flux is expressed as

$$\dot{q}_C = h_C(T_W - T_L)(1 - A_b), \quad (2)$$

where h_C is the heat transfer coefficient, and T_W and T_L are the wall and liquid temperatures.

The quenching heat flux \dot{q}_Q represents the heating of colder bulk liquid that fills the cavity left after periodic bubble departures. It is modelled as

$$\dot{q}_Q = \frac{2k_l}{\sqrt{(\pi\lambda_l T)}}(T_W - T_L), \quad (3)$$

where k_l is the conductivity, T is the periodic time between bubble departures, and $\lambda_l = \frac{k_l}{\rho_l c_{pl}}$ is the diffusivity. Evaporative heat flux is defined as

$$\dot{q}_E = V_d N_w \rho_v h_{fv} f, \quad (4)$$

where V_d is the volume of the departing bubbles, N_w is the active nucleation site density, ρ_v is the vapour density, h_{fv} is the latent heat of evaporation. And f is the bubble departure frequency. For boiling parameters Kocamustafaogullary and Ishii's model was used to model the bubble departure diameter (used to calculate V_d) and nucleation site density N_w [10], Cole model was used for the bubble departure frequency [11].

3.5 Interphase heat and mass transfer modelling

The heat transfer in mixture was modelled independently for each phase. From liquid to vapour heat transfer, the Hughmark model [12] was used, applicable for turbulent bubbly flows at a wide range of Reynolds numbers. To achieve saturation temperature of the liquid phase a zero-resistance condition was set for vapour to liquid heat transfer coefficient. This causes the interface temperature to always match the saturation temperature. Interfacial mass transfer (either condensation or evaporation) is directly correlated to interfacial heat transfer and can be written as

$$\dot{m} = \dot{m}_{lt} + \dot{m}_{vt} = \frac{q_{lt} + q_{vt}}{h_{fv}}, \quad (5)$$

where \dot{m}_{lt} is liquid vaporisation mass transfer rate, \dot{m}_{vt} is the vapour condensation mass transfer rate, q_{lt} is liquid to interphase heat flux and q_{vt} is vapour to interphase heat flux. They are calculated as a function of local temperature difference, interfacial area and an interphase constant. The vapour bubble diameter in the bulk liquid was modelled as a function of local subcooling [3].

3.6 Interfacial forces in momentum equations

To appropriately model the momentum exchange between the secondary (dispersed vapour bubbles) phase and the primary (liquid) phase, additional forces are added to the momentum equations. Those forces rely on the general formula and a model constant that can be calculated differently depending on the sub-model.

Drag forces account for interfacial drag between the continuous liquid phase and the vapour phase. For very small bubbles, they behave as solid spherical particles, driven by the liquid flow, but for larger bubbles, Reynold's numbers and surface tension effects become important. Ishii and Zuber's drag model used in the simulation [13], takes into account spherical bubble shapes in viscous regime and ellipsoidal or spherical capped bubbles in higher Reynolds number regimes.

Lift forces on the vapour phase bubbles are a consequence of the velocity gradients in the liquid phase flow. They are modelled as

$$\vec{F}_{lift} = -C_l \rho_q \alpha_p (\vec{v}_q - \vec{v}_p) \times (\nabla \times \vec{v}_q), \quad (6)$$

where C_l is the lift coefficient, ρ_q the primary phase density, α_p the secondary phase volume fraction, v_p the secondary phase velocity and v_q the primary phase velocity. For lift coefficient Moraga model was used [14].

Wall lubrication forces consider the effect of the wall on the bubbly flow. They tend to push the bubbles away from the wall. For vertical pipe flow this effect causes the bubbles to concentrate in the region near but not adjacent to the wall. In Fluent it is modelled as

$$\vec{F}_{wl} = C_{wl} \rho_q \alpha_p |(\vec{v}_q - \vec{v}_p)|_{\parallel} \vec{v}_{dr}, \quad (7)$$

where C_{wl} is the wall lubrication coefficient and \vec{n}_w normal to the wall. The model used was proposed by Tomiyama [15].

Turbulent dispersion force accounts for the interphase momentum transfer, that acts as a turbulent diffusion in dispersed flows. In a vertical boiling flow this is a main force that brings vapour from the wall to the centre of the pipe. It is modelled as a turbulent drag

$$\vec{F}_{t,dq} = -f_{td,lim} K_{pq} \vec{v}_{dr}, \quad (8)$$

where K_{pq} is interphase exchange coefficient, $K_{pq}\vec{v}_{dr}$ is turbulent dispersion force and $f_{td,lim}$ is a limiting factor. K_{pq} is always modelled as some sort of gradient of void fraction, in this simulation, Lopez de Bertodano model was used [16]. Model constant was adjusted from 1 to 5, to increase the bubble dispersion into the inner regions. A standard limiting function was used (as proposed in Fluent manual [3]).

4 RESULTS AND DISCUSSION

4.1 Model settings and boundary conditions

Case was set up with simple planar 2D axisymmetric geometry (see Figure 1). The pipe has a radius of 9.6 mm and the overall length of 5.5 m. Note, that the schematic representation of the pipe domain does not show the dimensions proportionally. The heated section is 3.485 (3.5m) long. A 1m long adiabatic section was added at the inlet side, so fully developed turbulent flow can enter the heated section. To keep the area of interest far from boundary layer, an adiabatic section was added at the end of the heated section as well. As in some other similar cases [1], a 1000×16 mesh was chosen. It was refined near the heated wall, as shown in the zoom-out in Figure1. Boundary values of the four simulated cases cases are presented in Table 1.

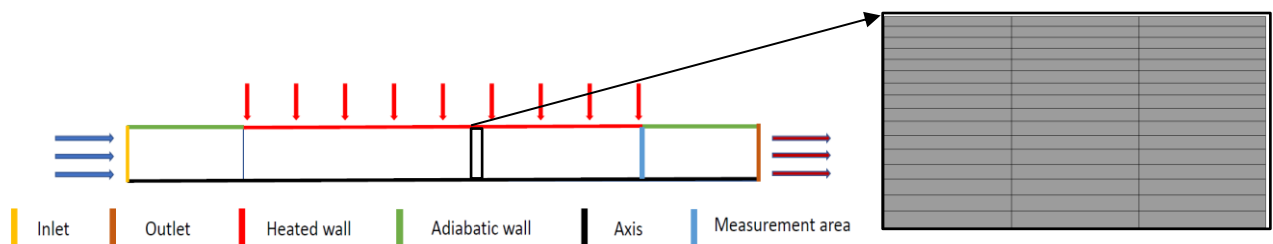


Figure 1: Case setup, boundaries and measurement section and zoom-out of the mesh.

The simulation was conducted using a pseudo transient solution method with phase coupled algorithm. Low enough time steps and adjustment of under-relaxation factors (URF) (see Table 2) was critical for achieving the converged solutions. It turned out that the density, body forces and vaporisation mass URF's were the most critical. Pseudo time step was selected automatically with the pre-set 0.01 factor. This meant the pseudo time step could be as low as 10^{-7} s at some critical moments, usually at the beginning of the simulation when the void fraction profiles were still developing, but in time this reduced to a more reasonable 10^{-3} s.

Table 2: Under-relaxations factors used in the simulation.

Quantity	Pressure	Momentum	Density	Body Forces	Vaporisation mass	Turbulence	Energy
URF	1	0.75	0.5	0.5	0.3	0.5	0.95

4.2 Simulation results

The results are shown at the end of the heated section (3.5m), where the measurements were performed. Figure background colour implies the sub-cooling, blue for high, purple for medium and light-red for low.

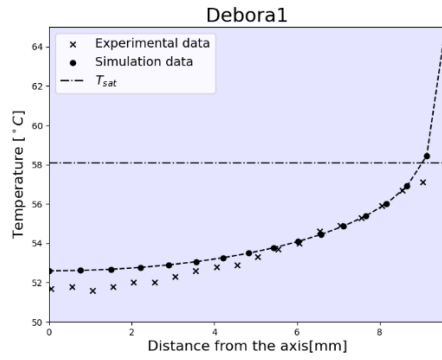


Figure 3: temperature profile in high subcooling case.

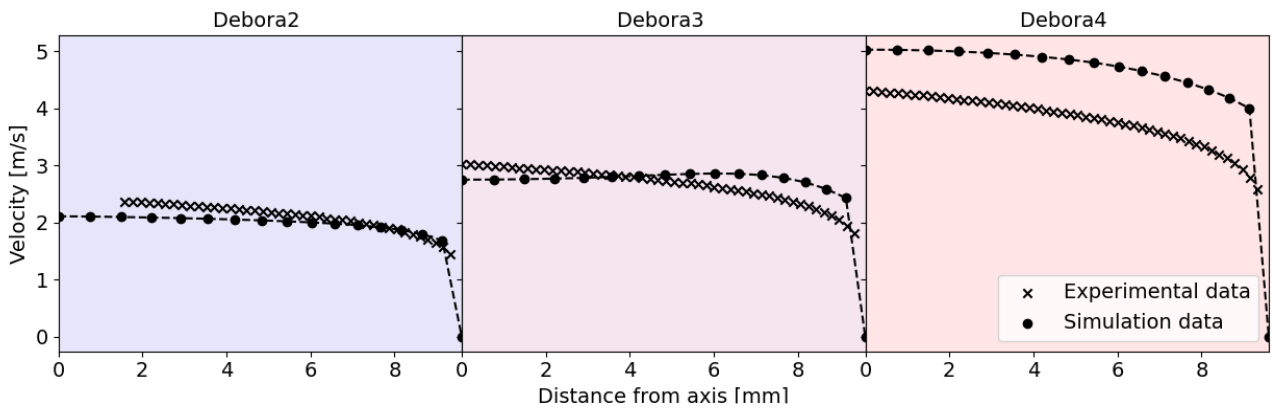


Figure 4: comparison of velocity profiles for simulated cases

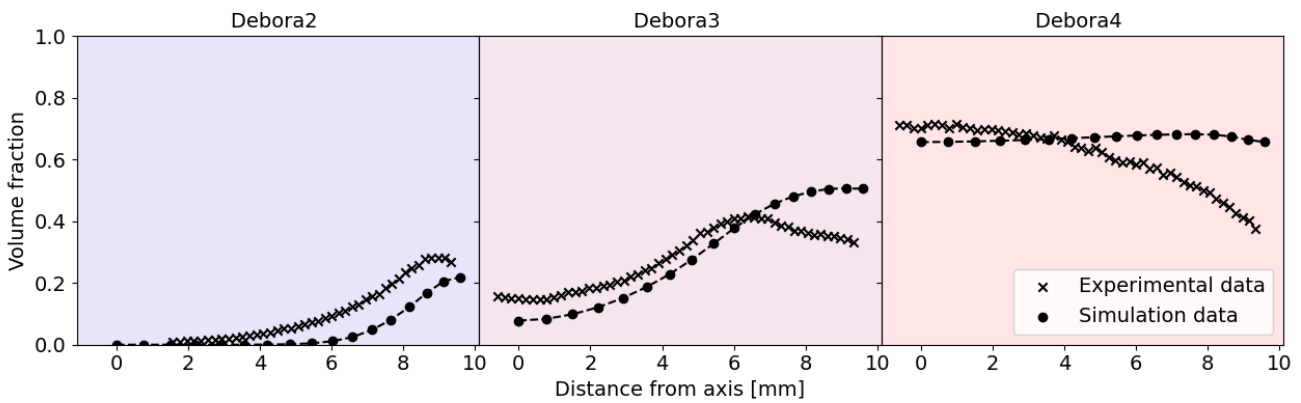


Figure 5: comparison of volume fractions for simulated cases.

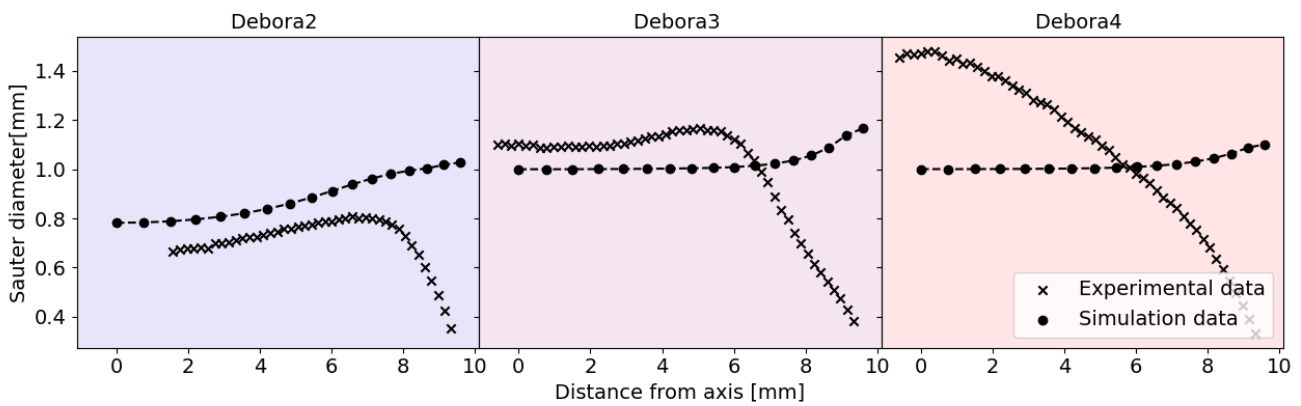


Figure 6: comparison of Sauter diameters for three simulated cases.

The simulations performed rather well at predicting the temperature of the liquid, as shown in Figure 3.

The velocity profiles shown in Figure 4 were close to the measured data, but as can be seen in Debora 4 case, the value was clearly overestimated by approximately 20%.

Volume fraction seems to be in reasonable proximity of the measured values, but as shown in Figure 5, the model in general failed in transferring enough vapour from the near the wall regions to the middle in all cases. This implies that a detailed parameter study on interfacial momentum forces should be conducted to understand the flow behaviour and to better match the experimental data. The value was also somewhat underestimated in the low temperature regime (Figure 5 left) and overestimated in the high temperature regime (Figure 5 right).

Sauter diameters followed the expected curve in inner pipe regions in low and medium temperature cases (Figure 6 left and centre), but completely failed at describing the behaviour in the near-wall regions and in high temperature case (Figure 6 right). Simulations by other authors [1,17], produced similar over-prediction of Sauter mean diameter in the near-wall regions, indicating that the discrepancy might be associated with some general limitation of the model in these regimes.

Overestimation of both velocity and volume fraction in the high temperature case could be attributed to the model's limitation in describing the saturated boiling flows. As A_b increases, a significant portion of the heat flux is transported directly to vapour phase. In that case vapour should heat up significantly and the used model (Equation 1) is not able to predict the on-going behaviour anymore. Non-equilibrium subcooled models are used for modelling flows from departure from nucleate boiling regime up to critical heat flux regimes [3].

Additionally, volume fraction profiles at different streamwise locations along the heated pipe were investigated. This could be useful to calibrate the model at other location along the channel, using the successfully simulated flow parameters at the measured location. On Figure 7, void volume fractions at different axial locations along the pipe can be observed. On the left a comparison of the predicted and experimental void fraction profiles at different axial locations of the boiling flow are shown, while on right the corresponding cross-section contours are presented. 2D cross section at different sections is shown. The area of the largest profile changes is also extended. The profiles at the lower locations could be also compared with the other available experimental profiles at higher axial locations, but at lower inlet sub-cooling.

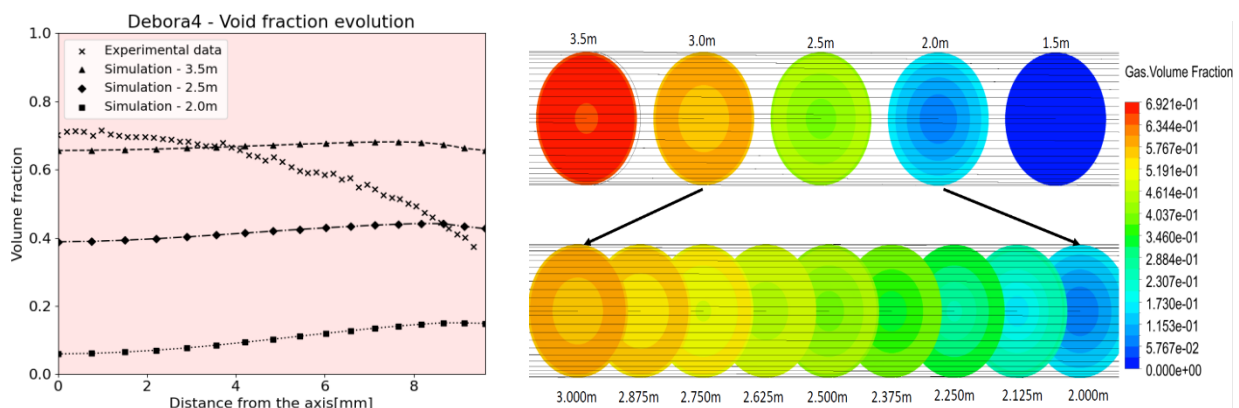


Figure 7 (Left) comparison of void fraction profiles at different sections along the pipe with the available experimental data. (Right) contours of volume fractions at different locations in the pipe.

CONCLUSIONS

In general, the preliminary simulations have demonstrated qualitatively reasonable prediction of boiling multiphase flow, especially considering the temperature and velocity profiles. Predictions of void fraction and bubble diameter profiles were less accurate, therefore detailed investigation and further validation of boiling and interphase transfer models is needed. Nevertheless, it cannot be expected that the existing models would be able to accurately predict all range of different boiling regimes with the increase inlet sub-cooling and void volume fraction, more advanced models will be needed to describe the phenomena near and beyond the saturated conditions.

ACKNOWLEDGMENTS

The financial support provided by the Slovenian Research Agency, grants L2-9210, P2-0405 and P2-0026 is gratefully acknowledged.

REFERENCES

- [1] Antoine Guelfi, Dominique Bestion, Marc Boucker, Pascal Boudier, Philippe Fillion, Marc Grandotto, Jean-Marc Hérard, Eric Hervieu & Pierre Péturaud (2007) NEPTUNE: A New Software Platform for Advanced Nuclear Thermal Hydraulics, Nuclear Science and Engineering, 156:3, 281-324, DOI: 10.13182/NSE05-98
- [2] J. Garnier, E. Manon, and G. Cubizolles. Local measurements on flow boiling of refrigerant 12 in a vertical tube. *Multiphase Science and Technology*, 13(1&2), 2001.
- [3] ANSYS Fluent Theory Guide, ANSYS, Inc., 275 Technology Drive Canonsburg, PA 15317, January 2021.
- [4] William E. Acree, Jr., James S. Chickos, "Isothermal Properties for Dichlorodifluoromethane (R12)" in NIST Chemistry WebBook, NIST Standard Reference Database Number 69, Eds. P.J. Linstrom and W.G. Mallard, National Institute of Standards and Technology, Gaithersburg MD, 20899, <https://doi.org/10.18434/T4D303>, (retrieved August 16, 2021). T.V. Vo, D. R. Edwards, "Development of In-Service Inspection Priorities fro PWR", *Nucl. Technol.*, 106, 1994, pp. 253-259.
- [5] F. R. Menter. "Two-Equation Eddy-Viscosity Turbulence Models for Engineering Applications". *AIAA Journal*. 32(8). 1598–1605. August 1994
- [6] A. A. Troshko and Y. A. Hassan. "A Two-Equation Turbulence Model of Turbulent Bubbly Flow". *International Journal of Multiphase Flow*. 22(11). 1965–2000. 2001.
- [7] Y. Sato and K. Sekoguchi. "Liquid Velocity Distribution in Two-Phase Bubbly Flow". *Int. J. Multiphase Flow*. 2. 79. 1979.
- [8] N. Kurul, M. Podowski, "On the modeling of multidimensional effects in boiling channels", *ANS Proc. 27th National Heat Transfer Conference*, Minneapolis, MN, pp. 28-31 (1991).
- [9] V. H. Del Valle and D. B. R. Kenning. "Subcooled flow boiling at high heat flux". *International Journal of Heat and Mass Transfer*. 28(10). 1907–1920. 1985.
- [10] G. Kocamustafaogullari and M. Ishii. "Foundation of the Interfacial Area Transport Equation and its Closure Relations". *International Journal of Heat and Mass Transfer*. 38. 481–493. 1995
- [11] R. Cole. "A Photographic Study of Pool Boiling in the Region of the Critical Heat Flux". *AIChE J.* 6.533–542. 1960.
- [12] G. A. Hughmark. "Mass and heat transfer from rigid spheres". *AICHE Journal*. 13. 1219–1221. November 1967.
- [13] M. Ishii and N. Zuber. "Drag Coefficient and Relative Velocity in Bubbly, Droplet or Particulate Flows". *AIChE J.* 25. 843-855. 1979.
- [14] F. J. Moraga, R. T. Bonetto and R. T. Lahey. "Lateral forces on spheres in turbulent uniform shear flow". *International Journal of Multiphase Flow*. 25. 1321–1372. 1999.
- [15] A. Tomiyama. "Struggle with computational bubble dynamics". *Third International Conference on Multiphase Flow*, Lyon, France. June 8–12, 1998.
- [16] M. Lopez de Bertodano. "Turbulent Bubbly Flow in a Triangular Duct". Ph.D. Thesis. Rensselaer Polytechnic Institute, Troy, New York. 1991.
- [17] Eckhard Krepper and Roland Rzehak. CFD for subcooled flow boiling: Simulation of DEBORA experiments. *Nuclear Engineering and Design*, 241(9):3851–3866, sep 2011.